



TITLE:

Ab initio study of ferroelectric closure domains in ultrathin PbTiO_3 films

AUTHOR(S):

Shimada, Takahiro; Tomoda, Shogo; Kitamura, Takayuki

CITATION:

Shimada, Takahiro ...[et al]. Ab initio study of ferroelectric closure domains in ultrathin PbTiO_3 films. Physical Review B 2010, 81(14): 144116.

ISSUE DATE:

2010-04

URL:

<http://hdl.handle.net/2433/129641>

RIGHT:

© 2010 The American Physical Society

Ab initio study of ferroelectric closure domains in ultrathin PbTiO_3 films

Takahiro Shimada,* Shogo Tomoda, and Takayuki Kitamura

Department of Mechanical Engineering and Science, Kyoto University, Sakyo-ku, Kyoto 606-8501, Japan

(Received 26 January 2010; published 16 April 2010)

Ab initio density-functional theory calculations within the local density approximation were conducted to elucidate whether critical thickness for ferroelectricity intrinsically exists in free-standing polydomain PbTiO_3 ultrathin films, where there was no screening effect of electrodes. The ferroelectric polydomain state was found to be energetically favorable over the paraelectric state even in the thinnest film one unit-cell thick, indicating no intrinsic critical thickness existed. The ferroelectric distortions in the film were stabilized by the formation of ferromagneticlike closure domains, because the surface charge, which caused a depolarizing field, was sufficiently screened by the in-plane aligned polarization at the surface. Further analysis of the covalent Pb-O bonding structure, which plays a central role in determining ferroelectricity in PbTiO_3 , revealed that the closure domain structure consists of the 180° as well as 90° domain walls.

DOI: [10.1103/PhysRevB.81.144116](https://doi.org/10.1103/PhysRevB.81.144116)

PACS number(s): 77.80.Dj, 31.15.A–, 68.60.–p

I. INTRODUCTION

Ferroelectric ultrathin films have drawn considerable attention because of their technological applications, e.g., non-volatile ferroelectric random access memory, transducers and electromechanical devices.^{1,2} Although these devices have so far employed films thicker than 100 nm under technological development, both the increasing demand for the miniaturization of devices and scientific interest in nanoscale ferroelectrics drives the investigation of fundamental ferroelectric properties in extremely thinner films of several atomic layers.

Ferroelectricity, which originates from the delicate balance between short-range covalent and long-range Coulomb interactions,^{3,4} is very sensitive to the size of materials (ferroelectric correlation volume).⁵ The existence of a critical size, where ferroelectricity vanishes, was first predicted on the basis of the classical Landau theory.^{6,7} In particular, the critical thickness of ferroelectric ultrathin films is of central interest in this discussion. For a ferroelectric thin film with a polar axis perpendicular to its surface, the termination of polarization at the surface or interface gives rise to surface charges. These surface charges create a depolarizing field that destabilizes the ferroelectric distortions.^{8,9} Two distinct ways to compensate for surface charges have traditionally been proposed: (i) screening by electrodes that accumulate surface charge at their interface⁹ and (ii) partitioning the system into domains.^{10,11}

In mechanism (i), theoretical studies^{12–15} based on *ab initio* density-functional theory (DFT) (Refs. 16 and 17) calculations have already been done for various ferroelectric ultrathin capacitors, with various combinations of ferroelectrics (BaTiO_3 and PbTiO_3) and electrodes (Pt and SrRuO_3). These studies revealed that, in a single-domain configuration, a critical thickness for ferroelectricity still exists, ranging from two to six unit cells depending on the choice of electrodes due to their different conductive behavior, chemical nature, and constraint of atomic displacement at the interface. Below the critical thickness, the system becomes paraelectric because of the insufficiency of screening by the electrodes. In recent years, Aguado-Puente and

Junquera,¹⁸ however, showed that the ferroelectric distortions in $\text{SrRuO}_3/\text{BaTiO}_3/\text{SrRuO}_3$ capacitors can be stabilized by breaking up the system into domains even below the critical thickness [mechanism (i) incorporated with (ii)].

In mechanism (ii), Fong *et al.*¹¹ experimentally showed that ferroelectricity is sustained in the PbTiO_3 film as thin as three unit-cell thick, which were epitaxially grown on an insulating SrTiO_3 substrate by forming 180° stripe domains. However, the critical thickness is expected to depend on the choice of substrate due to the different degree of constraint of displacement at the interface. To fundamentally understand the intrinsic critical thickness for ferroelectricity under mechanism (ii), it is essential to theoretically investigate a free-standing film, which is free from any substrate constraints.

In this paper, we investigated whether the critical thickness for ferroelectricity intrinsically exists in free-standing polydomain ultrathin PbTiO_3 films using *ab initio* density-functional theory calculations. In addition, the detailed ferroelectric domain structure of the ultrathin films was investigated from atomic and electronic points of view. The mechanism of stabilization of ferroelectricity in the ultrathin films is discussed, as well.

II. COMPUTATIONAL DETAILS

A. Simulation method

Ab initio (first-principles) calculations based on the density functional theory^{16,17} were conducted using the Vienna *ab initio* simulation package code.^{19,20} The electronic wave functions were expanded in plane-waves up to a cut-off energy of 500 eV. The electron-ion interaction was described by the projector augmented wave (PAW) potentials,^{21,22} which explicitly included the Pb $5d$, $6s$, and $6p$, the Ti $3s$, $3p$, $3d$, and $4s$, and the O $2s$ and $2p$ electrons in the valence states. The use of PAW potentials is essential for the computational efficiency as well as the accuracy of the all-electron scheme that avoids the problems due to the linearization of the core-valence exchange interaction. To evaluate the exchange-correlation energy, we employed the local density

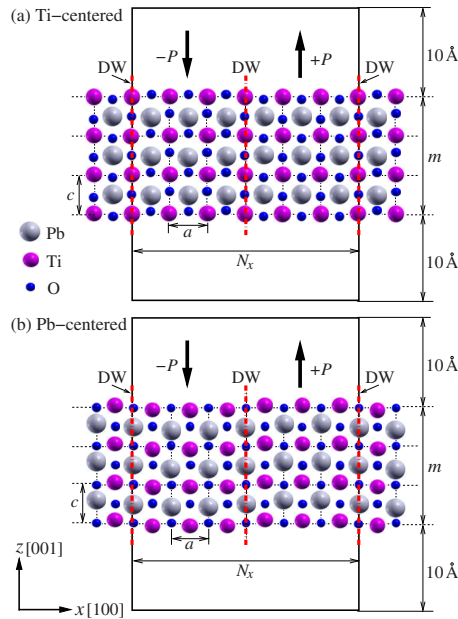


FIG. 1. (Color online) Simulation models of the free-standing PbTiO_3 ultrathin film with the TiO_2 -terminated (001) surfaces for the (a) Ti-centered and (b) Pb-centered 180° domain wall (DW) configurations. Spontaneous polarization, P , is initially set along the $+z$ and $-z$ directions on the right and left sides of the film, respectively. N_x and m denote the number of perovskite unit cells for the domain period and the thickness of film, respectively. The model shown here is $N_x=6$ and $m=3$. The solid boxes represent the simulation supercells.

approximation of the Ceperley-Alder form,²³ which successfully yielded the structural and ferroelectric ground-state of PbTiO_3 .^{14,24}

B. Simulation models and procedure

In this study, we investigate the free-standing polydomain PbTiO_3 ultrathin films with upward and downward spontaneous polarizations normal to the (001) surface. Figure 1 shows the simulation model of a three unit-cell thick ($m=3$) film with a domain period of six unit cells ($N_x=6$), where m and N_x denote the number of perovskite unit cells in the film thickness and the domain period, respectively. The films with a thickness of less than or equal to three unit cells ($m \leq 3$) were simulated in this study because the existence of a polydomain ferroelectric phase has already been observed experimentally in thicker films.¹¹ To study the ferroelectric stability with respect to the domain period, the models with different N_x were considered, as well. The TiO_2 termination was selected for the (001) surfaces of films because the termination is energetically favorable compared to another choice of the PbO termination.²⁵ Twinning on both the TiO_2 (Ti centered) and PbO (Pb centered) (010) planes was considered for the 180° domain wall (see Figs. 1(a) and 1(b), respectively). Since the three-dimensional periodic boundary condition was applied in the plane-wave pseudopotential calculations, a vacuum region of $l_v=20 \text{ \AA}$ was introduced in the z direction so that undesirable interactions from the neighboring films were sufficiently avoided. Thus, the simu-

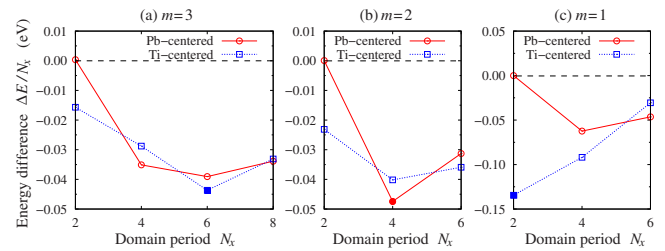


FIG. 2. (Color online) Total energy difference between the ferroelectric polydomain and paraelectric phases as a function of the domain period, N_x , for the (a) $m=3$, (b) $m=2$, and (c) $m=1$ unit-cell thick films with the TiO_2 -terminated (001) surfaces. Full symbols indicate the minimum for each film thickness.

lation cell dimensions in the x , y , and z directions were set to $N_x a$, a , and $mc + l_v$, respectively, where a and c are the theoretical lattice constants of the bulk, $a=3.867 \text{ \AA}$ and $c=4.034 \text{ \AA}$ ($c/a=1.043$). The Brillouin zone integrations were carried out using a $12/N_x \times 6 \times 2$ Monkhorst-Pack²⁶ k -point mesh with a Gaussian smearing of 0.20 eV , except for $N_x=8$ where a $2 \times 6 \times 2$ k -point mesh was used.

To obtain the equilibrated structure of the models, the atomic positions were fully relaxed using the conjugate-gradient method until all the Hellmann-Feynman forces were less than $2.5 \times 10^{-3} \text{ eV/\AA}$. The symmetry of inversion center in the domain walls was kept during the relaxation process.

Note that, because the net dipole moments in the simulation cell was completely cancelled out to be zero due to equivalent upward and downward spontaneous polarizations in the ferroelectric polydomain films, the periodic boundary condition produces no artificial external electric field, which would otherwise emerge in a single-domain film with a polarization perpendicular to its surface.²⁷

III. RESULTS AND DISCUSSION

A. Stability of ferroelectric polydomain phase in ultrathin PbTiO_3 films

Figure 2 shows the total energy difference between the ferroelectric polydomain and paraelectric phases, ΔE , as a function of the domain period, N_x , for films with thicknesses of 3, 2, and 1 unit cells. Here, the total energy difference was divided by N_x for a fair comparison among the different domain periods. In both the Pb- and Ti-centered three unit-cell thick films ($m=3$), the energy difference decreased with increasing domain period for $N_x \leq 6$, while it increased for $N_x \geq 6$. The stable domain period in the film was determined by an energetic competition between the advantage of the screening of depolarizing field by breaking the system into domains and the cost of the domain wall formation energy: a longer domain period lowers the energy cost to form domain walls, but leads to insufficient screening of the depolarizing field, and vice versa. The Ti-centered domain configuration with a period of $N_x=6$ was the most favorable for a film with $m=3$, due to its minimum energy. In addition, the negative energy difference indicates that the system prefers the ferroelectric polydomain state to the paraelectric state. This result

agrees with experimentally observed 180° stripe domain patterns of $N_x=6$ in a PbTiO_3 thin film of the same thickness ($m=3$) grown on SrTiO_3 ,¹¹ which supports the reliability of our DFT calculations.

For thinner films of $m=2$ and 1, the Pb-centered domain with a period of $N_x=4$ and the Ti-centered domain with an $N_x=2$ configuration, respectively, are energetically favored over the paraelectric state. It should be noted that the ferroelectric single-domain free-standing film was energetically unstable because of the existence of nontrivial depolarizing field,¹³ which brings the system back to a paraelectric configuration. This suggests that the depolarizing field in the films can be sufficiently cancelled out only by the formation of domains, even in the thinnest, one unit-cell thick ($m=1$) film, without any screening effect of electrodes. Therefore, no intrinsic critical thickness for ferroelectricity exists in free-standing ultrathin films.

We briefly mention that as the film thickness decreased ($m=3, 2$, and 1, respectively), the stable domain period became shorter ($N_x=6, 4$, and 2, respectively). This trend corresponds well with the experimentally observed relationship between film thickness and domain period in thicker films.¹⁰

B. Polarization distribution in polydomain PbTiO_3 films

The detailed ferroelectric domain structure in the ultrathin PbTiO_3 film is now investigated by introducing a site-by-site local polarization, \mathbf{P} , which can be evaluated by

$$\mathbf{P} = \frac{e}{\Omega_c} \sum_j w_j \mathbf{Z}_j^* \mathbf{u}_j, \quad (1)$$

where Ω_c , e , and \mathbf{u}_j denote the volume of the unit cell, the electron charge and the atomic displacement vector from the ideal lattice site of atom j , respectively. Index j covers all atoms in the unit cell. \mathbf{Z}_j^* is the Born effective charge tensor of cubic bulk PbTiO_3 . In this study, we employed the theoretical values of the Born effective charge tensors calculated by Zhong *et al.*⁴ The local polarization was evaluated for each Ti-edged unit cell in the film shown as dashed lines in Fig. 1. Weights were set to $w_{\text{Pb}}=1$, $w_{\text{Ti}}=1/8$, and $w_{\text{O}}=1/4$, which correspond to the number of unit cells sharing the atom. Note that this evaluation was previously validated²⁸ and has been applied to the nanostructures such as 90° domain walls^{28–30} and nanowires.³¹

Figure 3 shows the local polarization distribution in a three unit-cell thick film ($m=3$) of a stable Ti-centered domain having a period of $N_x=6$. Remarkably, a nontrivial in-plane polarization (in the x direction) was found near the junction between the surface and domain wall set initially [see red-colored values in Fig. 3(a)]. As a consequence, a closure domain structure, where polarization direction was aligned to form a closed flux, was formed in the film [see Fig. 3(b)]. Note that such closure domains were also formed in the thinner films of $m=2$ and 1, as well. The closure domains were first proposed in ferromagnetic systems by Landau and Lifshitz,³² and Kittel.³³ In recent years, however, Aguado-Puente and Junquera¹⁸ have theoretically proven the existence of closure domains in ultrathin $\text{SrRuO}_3/\text{BaTiO}_3/\text{SrRuO}_3$ ferroelectric capacitors. In our

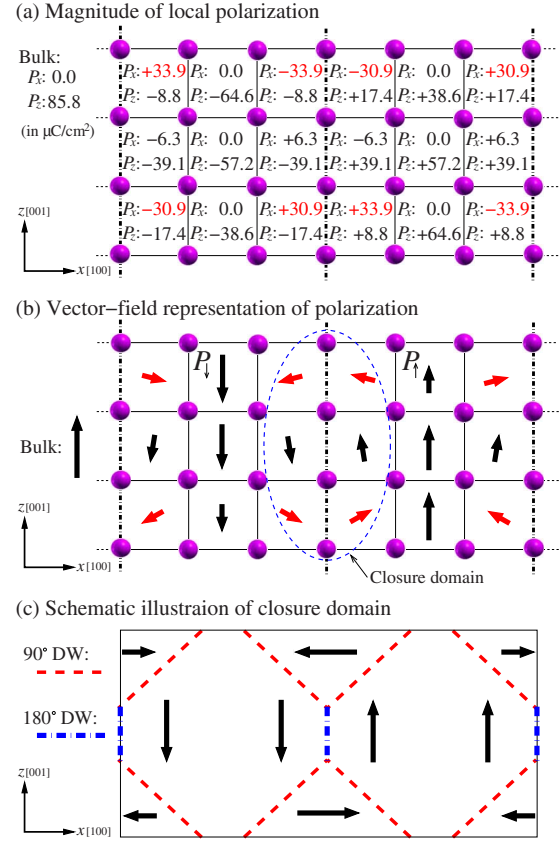


FIG. 3. (Color online) Local polarization distribution in a three unit-cell thick film ($m=3$) of a stable Ti-centered domain having a period of $N_x=6$: (a) magnitude of local polarization in the x and z directions, P_x and P_z . (b) Vector-field representation of local polarization. The purple spheres indicate Ti atoms. The vertical dotted-dashed lines indicate the initial position of 180° DWs. (c) Schematic illustration of the closure domain structure in the film consisting of the 90° and 180° domain walls. Arrows indicate the polarization direction in each domain.

model, the closure domain structure seems to consist of not only the 180° domain wall but also the 90° domain wall as Kittel proposed, which can clearly be seen in the vector field of the polarization distribution [see also Fig. 3(c) for a schematic illustration]. This will be discussed later, in terms of the covalent Pb-O bonding structure in the film. The formation of closure domains can considerably reduce the depolarizing field with respect to only the 180° domain wall configuration, because the in-plane polarization at the surface does not produce any surface charges.³³ Thus, more effective screening of the depolarizing field was realized by the formation of closure domains, which stabilized ferroelectric distortions in the ultrathin films.

On the other hand, the spontaneous polarization was along the normal z direction to the surface at the center of the domains, where there were two distinct cases of spontaneous polarization directed toward the (i) outside of the film, P_\uparrow , and (ii) inside of the film, P_\downarrow [see also Fig. 3(b) for the location]. The magnitude of polarizations, P_\uparrow and P_\downarrow , was reduced by about 55 % and 25 %, respectively, with respect to that of the bulk. This indicates that the presence of the surface suppressed the ferroelectricity. To be more precise,

TABLE I. Layer-by-layer ferroelectric distortion, δ (in Å), at the center of domain in a three unit-cell thick film ($m=3$) with a stable period of $N_x=6$. In parenthesis are the ratios to the bulk value. The results of a previous study (Ref. 34) of a free-standing single-domain PbTiO₃ film, in which the central layers were artificially fixed, are also shown for comparison. Cf. text.

Layer number	Center of domain in polydomain film		Single-domain film ^a	
	P_{\uparrow}	P_{\downarrow}	P_{\uparrow}	P_{\downarrow}
1 [TiO ₂]	-0.116 (-35%)	-0.202 (61%)	-0.108 (-32%)	-0.233 (70%)
2 [PbO]	0.366 (77%)	-0.244 (51%)	0.316 (66%)	-0.260 (55%)
3 [TiO ₂]	0.133 (40%)	-0.208 (63%)	0.153 (46%)	-0.201 (60%)
Bulk [TiO ₂]	0.333	-0.333	0.333	-0.333
Bulk [PbO]	0.476	-0.476	0.476	-0.476

^aReference 34.

we additionally introduced a layer-by-layer ferroelectric distortion, $\delta = \bar{z}_{\text{cation}} - \bar{z}_{\text{O}}$, where \bar{z} denotes the planar-averaged atomic position. Table I lists layer-by-layer ferroelectric distortions, δ , for the (001) planes of both the cells, P_{\uparrow} and P_{\downarrow} , shown in Fig. 3(b). Here, the topmost surface, second, and third layers are numbered 1, 2, and 3, respectively. The results of a previous DFT study³⁴ of a free-standing single-domain PbTiO₃ film five unit-cell thick, in which the center layers of the film were artificially fixed at the bulk state, are also shown for comparison. Overall, our result agrees reasonably well with the previous study of the single-domain film. For the case of P_{\downarrow} , δ was reduced by 40%–50% from the bulk value on both the TiO₂ and PbO layers. On the other hand, stronger suppression was found for P_{\uparrow} , especially, in the TiO₂ layers. In addition, the topmost surface TiO₂ layer exhibited a negative value of δ , suggesting that the surface relaxation led to an atomic shift in the direction opposite to the ferroelectric distortions of the bulk. Such an opposing shift of the surface TiO₂ layer results in a strong suppression of ferroelectricity for P_{\uparrow} .

C. Atomic and electronic structure of closure domains in ultrathin PbTiO₃ films

Figure 4 shows the atomic displacement from the paraelectric state in a three unit-cell thick film ($m=3$) of a stable Ti-centered domain having a period of $N_x=6$. The dis-

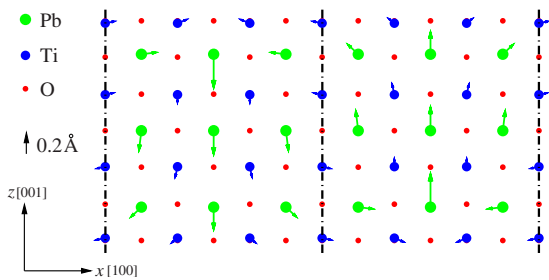


FIG. 4. (Color online) Atomic displacement from the paraelectric state in a three unit-cell thick film ($m=3$) of a Ti-centered domain having a stable period of $N_x=6$. Only the displacement of cations (Pb and Ti) is depicted for clarity. The vertical dotted-dashed lines indicate the initial position of 180° domain walls.

placement of atoms forms a closure-type flux across the domain wall. This displacement pattern corresponds well to the polarization orientation of closure domains described in the previous section. A similar closed-flux displacement pattern was observed in the thinner films with $m=2$ and 1. Remarkably, in-plane (the x direction) atomic displacement was found in the first and second surface layers of the film, which aligned the polarization parallel to the surface. In other words, the in-plane displacement played a significant role in the formation of closure domains, which stabilized the ferroelectric state in the film. In fact, the system turns back to the paraelectric state when the in-plane relaxation was neglected by constraining the x component of atomic coordinates. The displacement of closed flux was also observed in SrRuO₃/BaTiO₃/SrRuO₃ ferroelectric capacitors,¹⁸ when a closure domain was formed. It should be noted that only the displacement of Ti atoms was dominant in the SrRuO₃/BaTiO₃/SrRuO₃ capacitors, while the displacement of Pb atoms is much more active in the ultrathin PbTiO₃ film. This difference originates from the bonding nature of PbTiO₃ and BaTiO₃: the strong covalency of the Pb-O bond through the hybridization of the Pb 6s and O 2p orbitals plays a critical role in stabilizing large ferroelectric distortions in PbTiO₃,³⁵ while in BaTiO₃ only the Ti-O bond is responsible for ferroelectricity because of the ionic Ba-O interaction.³⁶ In fact, displacement of the Ba atom was inactive in SrRuO₃/BaTiO₃/SrRuO₃ capacitors. In addition, the covalent Pb-O bond often characterizes ferroelectricity in nanostructured PbTiO₃.^{29,31,35,37}

Figure 5 shows the atomic configuration and charge density distribution on the PbO (010) plane in a film three unit-cell thick ($m=3$). Those of the isolated 180° and 90° domain walls are also shown for comparison. Here, the covalent Pb-O bonds of interest are emphasized by white lines. For the single-domain bulk with the polar axis of [001], the Pb-O bond formed a zigzag shape along the [100] direction. In the film, on the other hand, this zigzag bonding structure was terminated and switched to the inverse structure across the center of area A (see the white solid lines). This bonding sequence was characteristically similar to that of the 180° domain wall, where the polarization direction changes from upward on one side to downward on the other. Meanwhile, a “ \sqsubset ”-type series of Pb-O bonds was found in the area B of

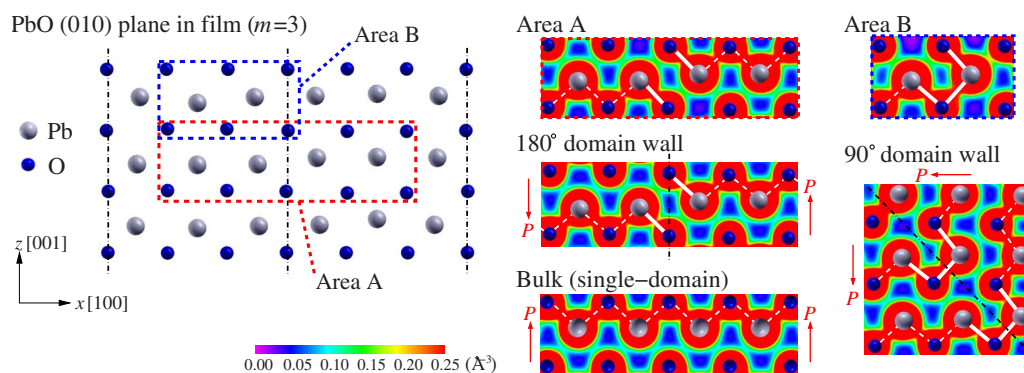


FIG. 5. (Color online) Atomic configuration and charge density distribution on the PbO (010) plane in a PbTiO_3 film three unit-cell thick ($m=3$) of a Ti-centered domain having a stable period of $N_x=6$. Those of the isolated 180° and 90° domain walls and the bulk are shown for comparison. Covalent Pb-O bonds are emphasized by white lines and solid and dashed lines indicate the Pb-O bonds observed near the domain walls and in the bulk, respectively. The dotted-dashed lines indicate the domain walls. Arrows, P , denote the polarization direction in each domain.

the film, which corresponds well to the bonding sequence in the 90° domain wall (see the white solid lines).²⁹ This indicates that the 180° and 90° domain walls were formed in the center of area A and in area B, respectively. Therefore, the closure domain structure in the PbTiO_3 film consists of both the 180° and 90° domain walls, as illustrated in Fig. 3(c).

IV. CONCLUSION

In this study, *ab initio* (first-principles) DFT calculations were performed to elucidate whether an intrinsic critical thickness for ferroelectricity exists in free-standing polydomain PbTiO_3 ultrathin films without any screening effect of electrodes. Moreover, the detailed ferroelectric domain structure of the ultrathin films was investigated from atomistic and electronic points of views to discuss the stabilization mechanism of the ferroelectric state in the films.

In a three unit-cell thick film ($m=3$), the ferroelectric polydomain state with the six unit-cell domain period ($N_x=6$) was found to be energetically favorable over the paraelectric state, which is consistent with experimentally observed 180° stripe domain patterns.¹¹ Further studies of the thinner films ($m=2$ and 1 unit-cell thick) revealed that the ferroelectric polydomain phase was also stabilized by the formation of domains with shorter periods of $N_x=4$ and 2,

respectively. This suggests that no critical thickness for ferroelectricity exists in free-standing polydomain films.

Local polarization analysis determined that the polarization direction aligned as a closed flux in the film. This indicates that a ferromagneticlike closure domain structure as first proposed by Kittel³³ was formed. Remarkably, in-plane atomic displacement was found in the surface layer, which leads to a nontrivial in-plane polarization component. Since the in-plane polarization does not induce surface charges, which would create a depolarizing field, the formation of a closure domain plays a central role in stabilizing the ferroelectric polydomain state in ultrathin film.

The charge density distributions indicated that the closed-flux displacement of Pb atoms leads to reconstruction of the covalent Pb-O bonds in the film. The resulting bonding structures at the center of the film and at the surface were found to be characteristically similar to the 180° and 90° domain walls, respectively. This indicates that the closure domain structure consists of both the 180° and 90° domain walls.

ACKNOWLEDGMENTS

This work was supported in part by a Grant-in-Aid for Scientific Research (S) (Grant No. 21226005) and a Grant-in-Aid for Young Scientists (B) (Grant No. 21760073), of the Japan Society of the Promotion of Science (JSPS).

*shimada@cyber.kues.kyoto-u.ac.jp

¹J. F. Scott, *Ferroelectric Memories* (Springer, Berlin, 2000).

²R. Ramesh, *Thin Film Ferroelectric Materials and Devices* (Kluwer Academic, Boston, 1997).

³R. Resta, M. Posternak, and A. Baldereschi, *Phys. Rev. Lett.* **70**, 1010 (1993).

⁴W. Zhong, R. D. King-Smith, and D. Vanderbilt, *Phys. Rev. Lett.* **72**, 3618 (1994).

⁵M. E. Lines and A. M. Glass, *Principles and Applications of Ferroelectrics and Related Materials* (Oxford University Press,

Oxford, 2001).

⁶R. Kretschmer and K. Binder, *Phys. Rev. B* **20**, 1065 (1979).

⁷W. L. Zhong, Y. G. Wang, P. L. Zhang, and B. D. Qu, *Phys. Rev. B* **50**, 698 (1994).

⁸I. P. Batra and B. D. Silverman, *Solid State Commun.* **11**, 291 (1972).

⁹R. R. Mehta, B. D. Silverman, and J. T. Jacobs, *J. Appl. Phys.* **44**, 3379 (1973).

¹⁰S. K. Streiffer, J. A. Eastman, D. D. Fong, C. Thompson, A. Munkholm, M. V. Ramana Murty, O. Auciello, G. R. Bai, and G.

- B. Stephenson, *Phys. Rev. Lett.* **89**, 067601 (2002).
- ¹¹D. D. Fong, G. B. Stephenson, S. K. Streiffer, J. A. Eastman, O. Auciello, P. H. Fuoss, and C. Thompson, *Science* **304**, 1650 (2004).
- ¹²J. Junquera and P. Ghosez, *Nature (London)* **422**, 506 (2003).
- ¹³N. Sai, A. M. Kolpak, and A. M. Rappe, *Phys. Rev. B* **72**, 020101(R) (2005).
- ¹⁴Y. Umeno, B. Meyer, C. Elsässer, and P. Gumbsch, *Phys. Rev. B* **74**, 060101(R) (2006).
- ¹⁵Y. Umeno, J. M. Albina, B. Meyer, and C. Elsässer, *Phys. Rev. B* **80**, 205122 (2009).
- ¹⁶P. Hohenberg and W. Kohn, *Phys. Rev.* **136**, B864 (1964).
- ¹⁷W. Kohn and L. Sham, *Phys. Rev.* **140**, A1133 (1965).
- ¹⁸P. Aguado-Puente and J. Junquera, *Phys. Rev. Lett.* **100**, 177601 (2008).
- ¹⁹G. Kresse and J. Hafner, *Phys. Rev. B* **47**, 558 (1993).
- ²⁰G. Kresse and J. Furthmüller, *Phys. Rev. B* **54**, 11169 (1996).
- ²¹P. E. Blöchl, *Phys. Rev. B* **50**, 17953 (1994).
- ²²G. Kresse and D. Joubert, *Phys. Rev. B* **59**, 1758 (1999).
- ²³D. M. Ceperley and B. J. Alder, *Phys. Rev. Lett.* **45**, 566 (1980).
- ²⁴Z. Wu, R. E. Cohen, and D. J. Singh, *Phys. Rev. B* **70**, 104112 (2004).
- ²⁵R. I. Eglitis and D. Vanderbilt, *Phys. Rev. B* **76**, 155439 (2007).
- ²⁶H. J. Monkhorst and J. D. Pack, *Phys. Rev. B* **13**, 5188 (1976).
- ²⁷B. Meyer and D. Vanderbilt, *Phys. Rev. B* **63**, 205426 (2001).
- ²⁸B. Meyer and D. Vanderbilt, *Phys. Rev. B* **65**, 104111 (2002).
- ²⁹T. Shimada, Y. Umeno, and T. Kitamura, *Phys. Rev. B* **77**, 094105 (2008).
- ³⁰T. Shimada, K. Wakahara, Y. Umeno, and T. Kitamura, *J. Phys.: Condens. Matter* **20**, 325225 (2008).
- ³¹T. Shimada, S. Tomoda, and T. Kitamura, *Phys. Rev. B* **79**, 024102 (2009).
- ³²L. Landau and E. Lifshitz, *Phys. Z. Sowjetunion* **8**, 153 (1935).
- ³³C. Kittel, *Phys. Rev.* **70**, 965 (1946).
- ³⁴M. Fechner, S. Ostanin, and I. Mertig, *Phys. Rev. B* **77**, 094112 (2008).
- ³⁵R. E. Cohen, *Nature (London)* **358**, 136 (1992).
- ³⁶Y. Kuroiwa, S. Aoyagi, A. Sawada, J. Harada, E. Nishibori, M. Takata, and M. Sakata, *Phys. Rev. Lett.* **87**, 217601 (2001).
- ³⁷Y. Umeno, T. Shimada, T. Kitamura, and C. Elsässer, *Phys. Rev. B* **74**, 174111 (2006).